Instabilities of a Gyroscope Produced by Rapidly Rotating, Highly Viscous Liquids

William P. D'Amico Jr.*
U.S. Army Armament Research and Development Center, Aberdeen Proving Ground, Maryland

A series of experiments was conducted to determine the yaw behavior of a gyroscope that contained a liquid-filled rotor. Spin rates, liquid viscosities, and cylinder geometries were selected to produce a wide range of Reynolds numbers ($5 < Re < 12{,}000$). Three cylinder aspect ratios (height-to-diameter) were tested: 1/1, 3/2, and 3/1. Coning frequencies for the free gyroscope were selected to be typical of spin-stabilized projectiles. Two distinct types of yaw behavior were observed with Reynolds number being the major controlling parameter. For $Re > 1000$, the motion of the gyroscope was reasonably well predicted by classical liquid-filled shell theories that postulate a resonance between a natural frequency of the spinning liquid and the yaw frequency of the gyroscope. For these conditions the maximum yaw growth rate will occur when an eigenfrequency of the liquid is approximately equal to the gyroscope yaw frequency. For cases where $Re < 1000$ the behavior of the gyroscope was not characterized by a resonant mechanism. Instead, the liquid-induced yaw moments and yaw growth rates grew monotonically with increasing yaw frequencies.

Nomenclature

a = radius of a right-circular cylindrical cavity containing liquid
C_{LIM} = liquid in-plane moment coefficient for one-mode coning or spiral motion; the imaginary part of C_{LM}
C_{LIM_j} = fast ($j=1$) and slow ($j=2$) mode liquid in-plane moment coefficients; the imaginary part of C_{LM_j}
C_{LM_j} = fast ($j=1$) and slow ($j=2$) mode liquid moment coefficients
C_{LRM} = $m_L a^2 \phi^2 \pi_1 K^2 C_{\mathrm{LRM}}$
C_{LSM} = liquid side moment coefficient for one-mode coning or spiral motion; the real part of C_{LM}
C_{LSM_j} = fast ($j=1$) or slow ($j=2$) mode liquid side moment coefficients; the real part of C_{LM_j}
$C_{M_{p_\alpha}}$ = |Magnus moment| / $\frac{1}{2}\rho S \ell^2 V \dot{\phi} |\tilde{\xi}|$
$C_{M_q} + C_{M_{\dot{\alpha}}}$ = |sum of the damping moments| $\div \frac{1}{2}\rho S \ell^2 V$ |cross spin|
C_{M_α} = |static moment| / $\frac{1}{2}\rho S \ell^2 V |\tilde{\xi}|$
C_{N_α} = $-$(normal force)/∞, $\rho S V^2 \tilde{\xi}$
c = one-half the length of the cylindrical cavity containing liquid
$\hat{H}$ = $(\rho S \ell / 2m)\,[C_{N_\alpha} - k_y^{-2}(C_{M_q} + C_{M_{\dot{\alpha}}})]$
h = distance from the gyroscope's pivot location to the center of the cylindrical cavity
I_x, I_y = axial and transverse moments of inertia of the gyroscope or projectile
K_j = magnitude of the jth yaw arm ($j=1,2$)
K_{j0} = initial value of K_j
k_x = $(I_y / m\ell^2)^{1/2}$, the projectile's axial radius of gyration
k_y = $(I_y / m\ell^2)^{1/2}$, the projectile's transverse radius of gyration
ℓ = reference length
$\tilde{M}$ = $(\rho S \ell^3 / 2I_y)(V/\ell)^2 C_{M_\alpha}$
$M_{L\tilde{Y}}, M_{L\tilde{Z}}$ = components of the aerodynamic moment
m = projectile mass
m_L = liquid mass in a fully filled cylindrical cavity
Re = $a^2 \dot{\phi} / \nu$, Reynolds number
S = reference area
s_g = $\sigma^2 \dot{\phi}^2 / 4\hat{M}$, the gyroscope stability factor
T = $(\rho S \ell / 2m)(V/\ell)\,[C_{N_\alpha} + k_x^{-2} C_{M_{p_\alpha}}]$
t = time
V = magnitude of the projectile's velocity vector
ϵ = nondimensionalized growth rate for single mode motion, $j=1$
ϵ_j = nondimensionalized growth rate of the jth yaw mode, ($j=1,2$)
ν = kinematic viscosity
$\tilde{\xi}$ = complex yaw in the nonrolling coordinate system
ρ = air density
σ = I_x / I_y
τ = τ_j for one-mode yawing motion
τ_j = $\phi_j / \dot{\phi}$, the nondimensionalized frequency of the jth yaw mode ($j=1,2$)
ϕ = $\dot{\phi} t$
ϕ_j = $\phi_{j0} + \tau_j \dot{\phi} t$ ($j=1,2$)
ϕ_{j0} = initial orientation angle of the jth yaw arm ($j=1,2$)
$\dot{\phi}$ = spin rate (assumed to be positive)

Superscripts

$(\vec{\ })$ = vector quantity
$(\dot{\ })$ = time derivative

Introduction

A SUBSTANTIAL amount of research has been conducted on the stability of the motion of spinning, liquid-filled containers. Areas of interest can be quite diverse. Two such examples are: liquid fuel cells on satellites or reentry vehicles and liquid-filled artillery projectiles. Most experience in rotating liquid flows is for cases where the rotational force is much large than the viscous force, i.e., high Reynolds

Presented as Paper 81-0224 at the AIAA 19th Aerospace Sciences Meeting, St. Louis, Mo., Jan. 12-15, 1981; submitted March 2, 1981; revision received Oct. 3, 1983. This paper is declared a work of the U.S. Government and therefore is in the public domain.

*Mechanical Engineer, Launch and Flight Division, Ballistic Research Laboratory, U.S. Armament, Munitions and Chemical Command. Member AIAA.

number (Re) flows. Typically, a Reynolds number is defined as $a^2\dot{\phi}/\nu$, where a is the radius of a cylindrical cavity, $\dot{\phi}$ the spin, and ν the kinematic viscosity of the liquid. This paper deals with a series of experiments that were conducted for $5<Re<12{,}000$. This range of Re has not been examined previously and is applicable to slowly spinning vehicles or highly viscous liquid payloads.

Stewartson[1] treated the stability of the motion of a liquid-filled top. In this analysis, an inviscid liquid was assumed to be spinning as a quasirigid body with the angular velocity of the top. It was determined that the yawing motion of the top could excite the natural frequencies of oscillation of the liquid (the eigenfrequencies) and a moment due to pressure disturbances within the liquid could destabilize the motion of the top. Wedemeyer[2] incorporated viscosity into the Stewartson theory through the use of boundary-layer-type corrections, and the Stewartson-Wedemeyer theory has compared favorably with gyroscope experiments conducted by Karpov.[3] Recent analyses by Murphy[4] and Gerber and Sedney[5] represent more complete and rigorous models than the Stewartson-Wedemeyer theory, but all of these treatments are still limited to "high Reynolds numbers" due to viscous corrections at the walls of the container.

For low Reynolds number rotating flows, D'Amico and Miller[6] observed large yaw and despin moments. Miller conducted laboratory experiments using a fixed precession angle spin fixture and determined despin moments over a wide range of Reynolds number.[7] D'Amico fired yawsonde-instrumented projectiles which produced rapid yaw growth and violent despin histories for approximately that same range of Reynolds numbers.[8,9] This report describes a series of laboratory experiments where the liquid-induced yaw moment was measured as a function of the yawing frequency of a gyroscope. The spin of the gyroscope was held constant (no despin moments will be reported), and the yawing motion of the gyroscope was less than 5 deg. The Reynolds number range for these data is $5<Re<12{,}000$. Comparisons of liquid-induced yaw moment coefficients for flight and gyroscope tests are made. Correlations for the liquid-induced yaw moment with pertinent dimensionless groups are made. Also, a lower bound in Reynolds number was tentatively established for the application of viscous corrected theories such as Murphy[4] and Gerber and Sedney.[5]

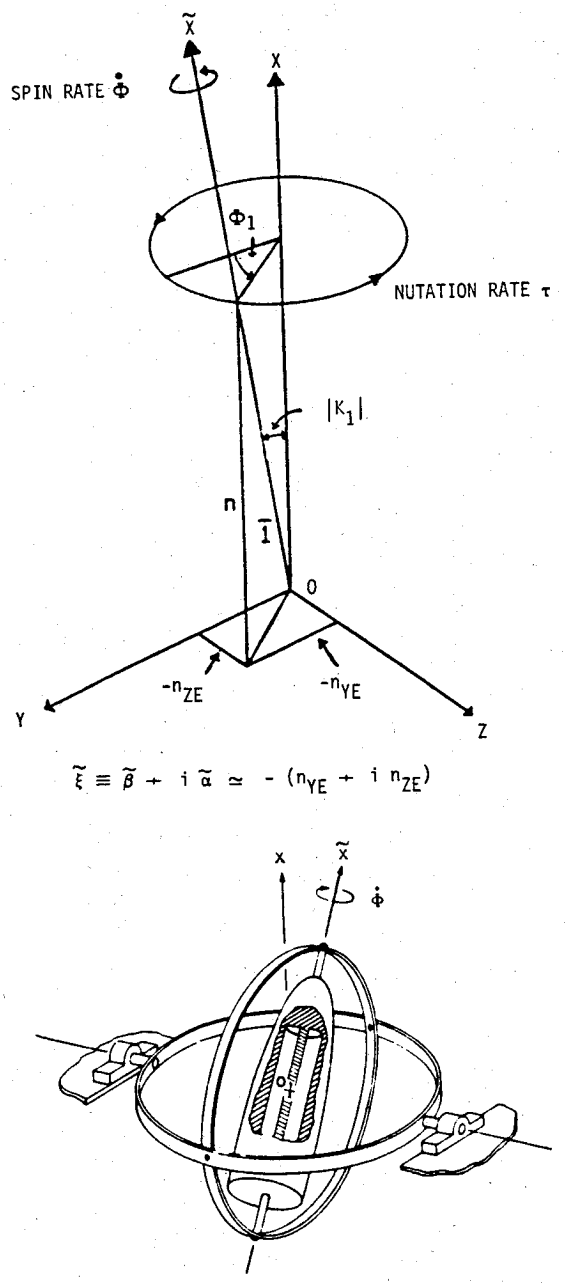

Fig 1 Schematic of gyroscope system.

Laboratory Gyroscope

Simulation of a Spin-Stabilized Projectile with a Gyroscope

A freely gimbaled gyroscope similar to that used by Karpov[3] was used to measure the yaw moments produced by a highly viscous rotating liquid. A short explanation of the dynamical behavior of the gyroscope will aid in the interpretation of the test data (see Fig. 1). A spin-stabilized projectile experiences a complicated angular motion during free flight. Only certain aspects of this free-flight motion will be simulated by the gyroscope. For the case of a projectile which does not contain a liquid and where the affects of drag are neglected,[4] the angular motion is described by

$$\ddot{\tilde{\xi}} + (\hat{H} - i\sigma\dot{\phi})\dot{\tilde{\xi}} - (\hat{M} + i\sigma\dot{\phi}\hat{T})\tilde{\xi} = 0 \tag{1}$$

where $\tilde{\xi}$ is the complex yaw within a nonrolling coordinate system and

$$\hat{H} = \text{damping moment} = (\rho S\ell/2m)\left[C_{N_\alpha} - k_y^{-2}(C_{M_q} + C_{M_{\dot{\alpha}}})\right]$$

$$\hat{M} = \text{static moment} = (\rho S\ell^3/2I_y)\,C_{M_\alpha}\,(V/\ell)^2$$

$$\hat{T} = \text{Magnus moment} = (\rho S\ell/2m)\left[C_{N_\alpha} + k_x^{-2}C_{M_{p_\alpha}}\right](V/\ell)$$

$$\dot{\phi} = \text{spin rate}$$

$$\sigma = I_x/I_y$$

If an epicyclic motion is assumed for the empty projectile, then,

$$\tilde{\xi} = K_1 e^{i\phi_1} + K_2 e^{1\phi_2} \tag{2}$$

where ordinarily

$$K_j = K_{j0}e^{\epsilon_j\dot{\phi}_j t}, \qquad j = 1,2 \tag{3}$$

$$\dot{\phi}_j = \dot{\phi}_{j0} + \tau_j\dot{\phi}_j t \tag{4}$$

$$\tau_j = (\sigma/2)\left(1 \pm \sqrt{1 - 1/s_g}\right) \tag{5}$$

where s_g is the gyroscopic stability factor, I_x and I_y the axial and transverse moments of inertia, respectively, and τ_1 and τ_2 are the fast and slow yaw frequencies, respectively. (A spin-

tabilized projectile has two modes of precession or yaw.) Explicit forms for the yaw growth rate ϵ_j and th gyroscopic tability factor are

$$\epsilon_j = -(\tau_j \hat{H} - \sigma \hat{T}) / [(2\tau_j - \sigma)(\tau_j \dot{\phi})] \tag{6}$$

$$s_g = \sigma^2 \dot{\phi}^2 / 4\hat{M} \tag{7}$$

A gyroscope has a gravity moment $\hat{G}$ that acts in a similar ashion as the static moment $\hat{M}$. Experience with the yroscope has shown that both precessional modes will damp hen the center of mass is slightly below the gimbal pivots; or this configuration $\hat{G}<0$. The direction of $\dot{\phi}_1$ will be the ame as $\dot{\phi}$, while the direction of $\dot{\phi}_2$ will be opposite to $\dot{\phi}$. The yroscope stability factor will be negative since $\hat{G}<0$. Iowever, $|s_g| \gg 1$, and for the empty gyroscope,

$$\tau_1 \cong \sigma \quad \text{and} \quad \tau_2 \cong 0 \tag{8}$$

Typically, the gyroscope is operated such that $.04<\tau_1<0.10$ and $|\tau_2|<0.005$, which corresponds to the onditions set out in Eq. (8).

A form for the liquid moment has also been suggested by lurphy.[4] It is assumed that the fast and slow yaw modes are ecoupled and that each component is proportional to $\tau_j K_j$ a linear formulation).

$$M_{L\hat{Y}} + iM_{L\hat{Z}} = m_L a^2 \dot{\phi}^2 [\tau_1 C_{\mathrm{LM}_1} K_1 e^{i\phi_1} + \tau_2 C_{\mathrm{LM}_2} K_2 e^{i\phi_2}] \tag{9}$$

here the liquid moment was scaled by the liquid mass, m_L; ne cylinder radius, a; and the spin, $\dot{\phi}$. This internal liquid ioment can be incorporated into the projectile description rovided by Eq. (1), yielding

$$\ddot{\tilde{\xi}} + (\hat{H} - i\sigma\dot{\phi})\dot{\tilde{\xi}} = (\hat{M} + i\sigma\dot{\phi}\hat{T})\tilde{\xi}$$

$$= i\dot{\phi}^2 (m_L a^2 / I_y) [\tau_1 C_{\mathrm{LM}_1} K_1 e^{i\phi_1} + \tau_2 C_{\mathrm{LM}_2} K_2 e^{i\phi_2}] \tag{10}$$

C_{LM_j} will ultimately depend upon many variables (K_j, τ_j, $_j$, Re, c/a), but a simple form from Ref. 4 will be used when he spin is positive.

$$C_{\mathrm{LM}_j} = C_{\mathrm{LSM}_j} + iC_{\mathrm{LIM}_j} \tag{11}$$

C_{LSM_j} is a side moment coefficient that controls the projectile aw damping, while C_{LIM_j} is an in-plane moment coefficient hat principally modifies the frequency of motion.

General expressions for yaw frequencies and yaw growth or damping) rates can be obtained from Eqs. (10) and (11):

$$\tau_j = (\sigma/2)[f_j - (-1)^j \sqrt{f_j^2 - (1/s_g)}] \tag{12}$$

or

$$f_j = 1 + (m_L a^2 / I_x) C_{\mathrm{LIM}_j}$$

nd

$$\epsilon_j = (m_L a^2 / I_x)(2\tau_j/\sigma - 1)^{-1} C_{\mathrm{LSM}_j} \tag{13}$$

Equations (12) and (13) can be inverted to obtain ex- ressions for C_{LIM_j} and C_{LSM_j} based upon experimentally determined values of ϵ_j and τ_j. During the course of the experiments it was observed that τ_1 for the liquid-filled gyroscope was within 1% of τ_1 for the empty gyroscope. This small difference is the effect of C_{LIM} on τ_1. Attempts were made to utilize this small difference between the liquid-filled and empty coning frequencies to establish C_{LIM_1} values. It was found that the frequency measurements were not sufficiently accurate to predict C_{LIM_1}. Equation (13) will be used to determine C_{LSM_1}. Other assumptions are valid for the gyroscope and can be used to simplify the above equations. First, damping rates for the empty gyroscope are very small (typically $\epsilon_j \leq -5\times10^{-3}$). Hence, the only moment acting on the gyroscope will be that produced by the liquid. Also, the yawing motion will be assumed to consist of only the fast yaw mode; i.e., $\hat{\xi} = K_1 e^{i\phi_1}$. It is assumed that the stability of the gyroscope is controlled by the liquid, and the motion is dominated by the fast yaw mode. As such, the dimensioness fast yawing frequency will be referreed to as the coning frequency, i.e., $\tau = \tau_1$, and the yaw growth rate of the fast mode is redefined as $\epsilon_1 = \epsilon$. For $\tau = \sigma$ and $\hat{H} = \hat{T} = 0$, Eq. (13) becomes

$$C_{\mathrm{LSM}} = \epsilon / (m_L a^2 / I_x) \tag{14}$$

The above formulation also assumes that ϵ is relatively small. For the experimental data presented here $\epsilon < 0.02$ and Eq. (14) can be used.

Table 1 Cylinder dimensions

Cylinder type	Height, cm	Diameter, cm	Aspect ratio, c/a	Offset, cm
1/1	13.246	12.718	1.042	−1.530
3/2	18.854	12.690	1.486	+5.887
3/1	25.768	8.242	3.126	−0.949

Operation of a Liquid-Filled Gyroscope

Cylindrical containers are located within the rotor of a freely gimbaled gyroscope. The inner gimbal supports the rotor and the test cylinders. Weights can be located on the rotor to control I_x. Weights can also be attached to the top or bottom of the inner gimbal. During the course of a test run, a dc motor (located beneath the inner gimbal) drives the rotor at a constant rate. The positions of the weights located on the inner gimbal can be moved to vary I_y, and these weights are used to control I_x/I_y, which from Eq. (8) provides control of the coning frequency. As previously stated, the center of gravity of the rotor/inner gimbal is slightly below the support pivots. The pivots consist of crossed spring leaves (so called flexural pivots) instrumented with strain gages. With the aid of usual bridge circuit techniques, strain is calibrated as a function of deflection. The response of the measurement system is linear for deflections up to 10 deg.

The yaw of the gyroscope is the angle between the vertical and the spin axis of the rotor. The liquid is allowed ample time to achieve a state of rigid-body rotation prior to the rotor being released. The inner gimbal is released from the vertical position without any initial disturbance. Unstable motion, if it occurs, is normally self starting from the vertical position. The yawing histories for each set of experiments are digitized and passed to a computer. The computer processes the yaw record to determine a K_1 history. An initial amplitude is determined, K_{10}, and is used as a reference by which all successive K_1 values are scaled. The ratio $[\ln(K_1/K_{10})]$ is displayed vs the time. A linear variation of $\ln(K_1/K_{10})$ indicates a constant growth rate for exponential variations in K_1. The data are fit by a linear least-squares technique to determine the growth rate. Three cylinders were tested. Height ($2c$), diameter ($2a$), aspect ratio (c/a), and offset (h) of the geometric center of the cylinder from the gimbal pivots are listed in Table 1.

The cylinders are referenced by their approximate aspect ratio which corresponds to the cylinder type as listed above. Silicone oils were used as test fluids. The kinematic properties of these oils are given in Table 2.

Water has a kinematic viscosity of approximately 1 cs = 0.01 cm^2/s under standard conditions. Most of the data were taken at a spin rate of 50 Hz; however, some data trials were made at 33.3, 41.6, or 58.3 Hz. For a particular cylinder, viscosity, and spin, the stability of the gyroscope was

measured over a wide range of coning frequencies. For the higher viscosity oils, a rapid survey at three coning frequencies was used, while for the lower viscosity oils, a dense survey of coning frequencies was made to produce a detailed response curve. In summary, the parameters that were varied during the experiments were: cylinder aspect ratio, c/a; kinematic viscosity, ν; spin rate, $\dot{\phi}$; and coning frequency, τ. Control of these quantitites produced the following parameter ranges: $5 < Re < 12{,}000$ and $0.04 < \tau < 0.1$.

Liquid-Filled Gyroscope Experiments

Two objectives were outlined for the gyroscope tests: 1) to determine the yaw moments produced for low Reynolds numbers and 2) to determine the validity of linear models that utilize boundary-layer corrections[4,5] as a function of Reynolds number. The liquid moment will have a complicated behavior, but the primary independent variables are Re, c/a, τ, K_I, and ϵ. In the present experiments for $Re < 12{,}000$, linear growth rates were observed for $K_I < 5$ deg. The basic measurement of a yaw growth rate will normally be converted into C_{LSM}. The use of C_{LSM} will also allow for the comparison fo the gyroscope data with existing flight data. C_{LSM} is usually presented as a function of the coning frequency τ or the product $Re \cdot \tau$, which is a Reynolds number whose characteristic frequency is based upon the fast yaw frequency $\dot{\phi}_I$ rather than the spin rate $\dot{\phi}$.

An estimation of experimental errors for the gyroscope data was not specifically performed; rather, multiple runs for the same set of test conditions were recorded and analyzed. All of these runs are provided, thus indicating the repeatability of the entire measurement and data reduction procedure.

The wide range in Reynolds number is achieved primarily by the choice of the viscosity of the liquid. For $Re > 5000$, the aspect ratios of the 1/1 and 3/1 cylinders were selected such that τ was sufficiently close to an eigenfrequency to produce unstable yawing motion. (The aspect ratio of the 3/2 cylinder was specifically chosen not be close to an eigenfrequency and, therefore, would have a stable yawing motion for large Re.) Comparisons between experimental data and models that use boundary-layer viscous-type corrections should be good for "large Reynolds numbers." Figure 2 provides such a comparison for the 1/1 cylinder when $Re = 12{,}400$. Within Ref. 4 growth rate predictions were made for incremental changes in c/a. A slightly better correlation with the experimental data was obtained when the computational aspect ratio was increased by 0.5%. Figure 2 does not include predictions of growth rate for slightly modified c/a values. Figure 3 shows comparisons of theory and experiment for $c/a = 1/1$ for $Re = 1260$. It is not clear whether the differences between the observed and predicted growth rates are due to small measurement errors in c/a or increased viscous forces. However, the agreement is still sufficiently good for practical applications. Figures 4 and 5 present comparisons for the 3/1 cylinder when $Re = 5210$ and 1010. The agreement between experiment and theory is not good. Within Ref. 4 comparisons of theory and experiment were substantially better for $Re = 9{,}000$ and 520,000. All of the data in Figs. 2-5 have a similar character: nonmonotonic dependence of growth rate with coning frequency. For $Re < 1000$, the nature of the response curve (for the same range in coning frequency) changes dramatically. Experimental data for these cases will be presented in the form of a liquid side moment coefficient (C_{LSM}) rather than growth rate to allow a comparison with flight data.

Data for a Viscosity Ratio of 10,000

A large number of experiments were performed to obtain C_{LSM} vs τ for a viscosity ratio of 10,000. It was observed that C_{LSM} was nearly linear with τ for all cases. Small changes in Re were obtained by different spin rates. Changes in C_{LSM} that were produced by variations in spin were correlated by using $Re \cdot \tau$ rather than simply τ, as seen in Fig. 6. However, C_{LSM} data for different aspect ratios (but identical spin rates) were not well correlated by $Re \cdot \tau$.

Table 2 Fluid properties

Viscosity ratio (ν/ν_{water})	Kinematic viscosity, cs	Density, g/cm^3
100	102.4	0.972
500	528.6	0.972
1,000	1,004.5	0.974
10,000	9,468.5	0.953
60,000	58,955	0.960
100,000	101,772	0.963

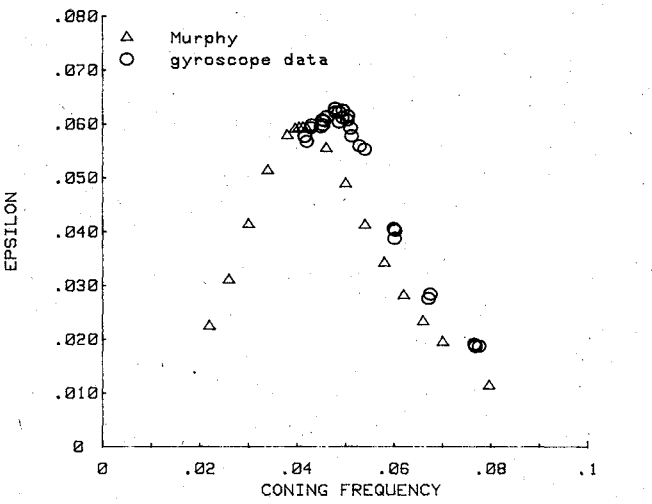

Fig. 2 Comparison of theory by Murphy[4] and gyroscope data: fill ratio 100%, $c/a = 1.042$, $Re = 12{,}400$, $I_x = 7.94 \times 10^5$ g·cm^2, $n = 1$, $j = 0$.

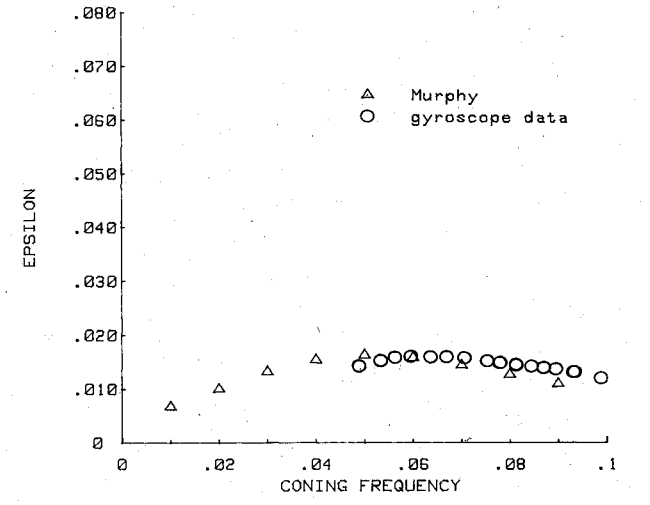

Fig. 3 Comparison of theory by Murphy[4] and gyroscope data: fill ratio 100%, $c/a = 1.042$, $Re = 1260$, $I_x = 10.46 \times 10^5$ g·cm^2, $n = 1$, $j = 0$.

Data for a Viscosity Ratio of 60,000

Experiments were also conducted to determine C_{LSM} vs τ for a viscosity ratio of 60,000. As before, it is observed that C_{LSM} is linear with τ and that small variations in spin can be correlated by using $Re \cdot \tau$. Figure 7 shows a data correlation of different aspect ratios for a single spin rate.

Data for a Viscosity Ratio of 100,000

Figure 8 gives data for a viscosity ratio of 100,000. Very little data were taken since the gyroscope was often stable. A linear variation of C_{LSM} with τ is observed.

Correlation of Data for Viscosity Ratios of 10,000, 60,000 and 100,000

A large volume of data now exists for low Re liquid moment coefficients. All of the data are shown in Fig. 9 with $Re\cdot\tau$ as the correlation parameter. It was anticipated that a good correlation would not occur for all variables. The expanded scale has artificially enhanced the correlation and has clustered data for each viscosity ratio (for exmple, all of the data for $Re\cdot\tau>4$ are for a viscosity ratio of 10,000). The C_{LSM} data were plotted against combinations of $(Re, \tau, c/a)$. A correlation for $C_{LSM}=0.0125+0.0756\ (Re)\ (\tau^2)\ (c/a)^{-1}$ was selected by a linear least-squares fit and is presented in Fig. 10. Several deficiencies are obvious. First, much of the data for very low Re were collapsed near the origin. However, the larger (and potentially destabilizing) values of C_{LSM} were well correlated.

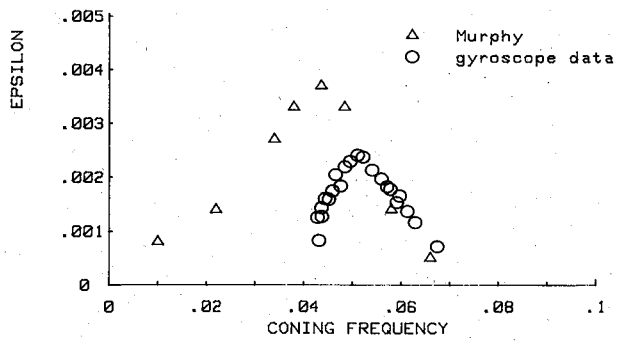

Fig. 4 Comparison of theory by Murphy[4] and gyroscope data: fill ratio 100%, $c/a=3.126$, $Re=5210$, $I_x=8.23\times10^5$ g·cm^2, $n=1$, $\tau=1$.

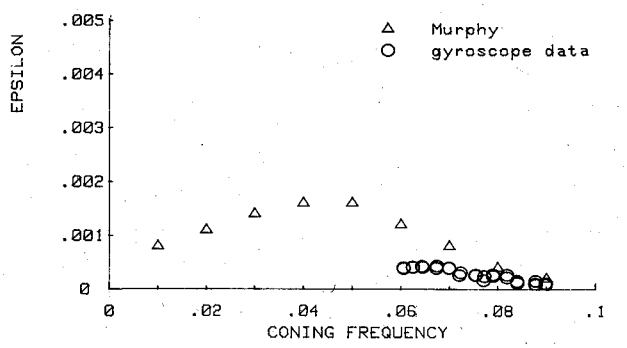

Fig. 5 Comparison of theory by Murphy[4] and gyroscope data: fill ratio 100%, $c/a=3.126$, $Re=1010$, $ZI_x=10.76\times10^5$ g·cm^2, $n=1$, $\tau=1$.

Comparison with Flight Data

Flight data from projectiles are available within Refs. 8 and 9. Unfortunately, flight data and gyroscope data are not at the same aspect ratio and Reynolds number, although new tests are planned to match flight and gyroscope conditions. Yawsonde data were processed for C_{LSM} in a fashion similar to that of the gyroscope data. The amplitude of the yaw was greater than that of the gyroscope. The effects of aerodynamic damping were neglected, but the flight Mach numbers were transonic and under such conditions the aerodynamic damping of the projectile is small. Figure 11 shows a comparison between flight data (Ref. 9, round E1-9542) and gyroscope data for comparable Reynolds numbers. Figure 12 shows a second comparison between flight data (Ref. 8, round E1-9396) and gyroscope data. Due to the differences in both Re and c/a comparisons may not be valid. However, the flight and gyroscope determined C_{LSM} data are similar in both cases. The data in Fig. 11 show a consistent trend in τ, but this did not occur in Fig. 12. A data comparison for a wide range of τ would be difficult since projectiles normally have $\tau\sim0.08$. The flight data also can be

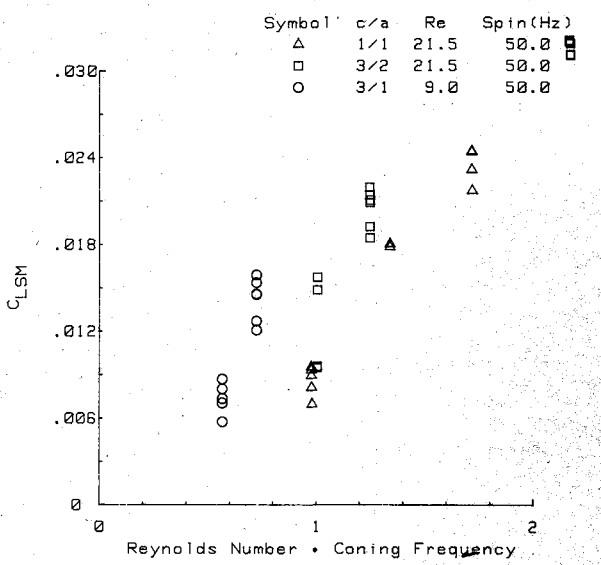

Fig. 7 Liquid side moment coefficient (C_{LSM}) vs $Re\cdot\tau$ for c/a's of 1/1, 3/2, and 3/1 with a viscosity ratio of 60,000.

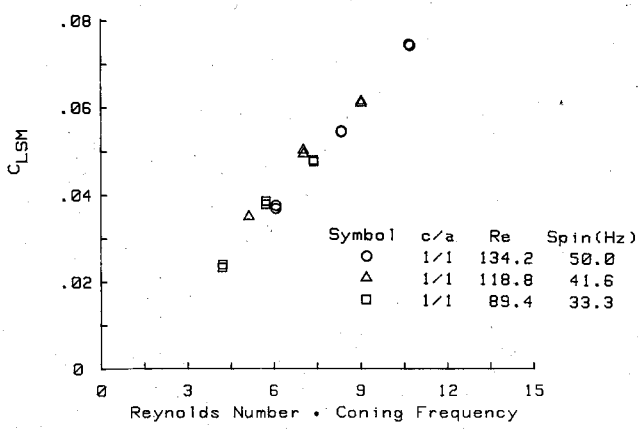

Fig. 6 Liquid side moment coefficient (C_{LSM}) vs $Re\cdot\tau$ for c/a of 1/1 with a viscosity ratio of 10,000.

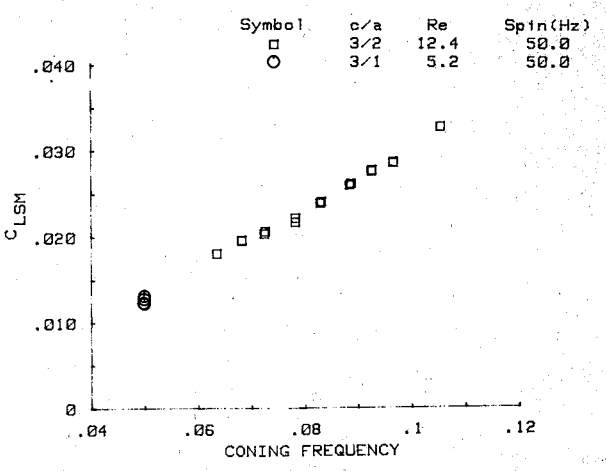

Fig. 8 Liquid side moment coefficient (C_{LSM}) vs coning frequency τ for c/a's of 3/1 and 3/2 and a viscosity ratio of 100,000.

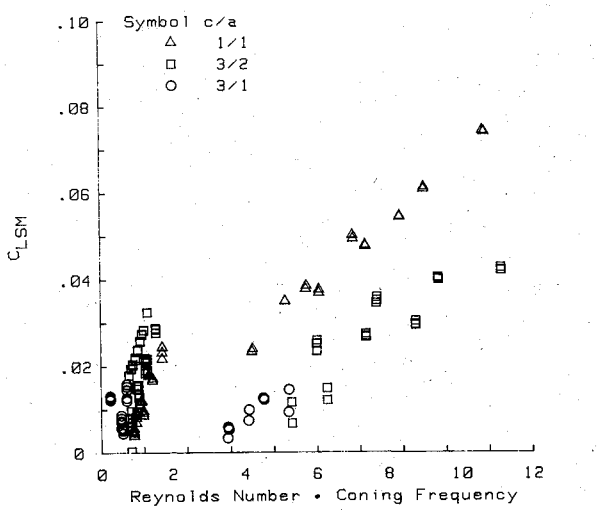

Fig. 9 Correlation of all data with viscosity ratios of 100,000, 60,000, and 10,000 for C_{LSM} vs $Re \cdot \tau$.

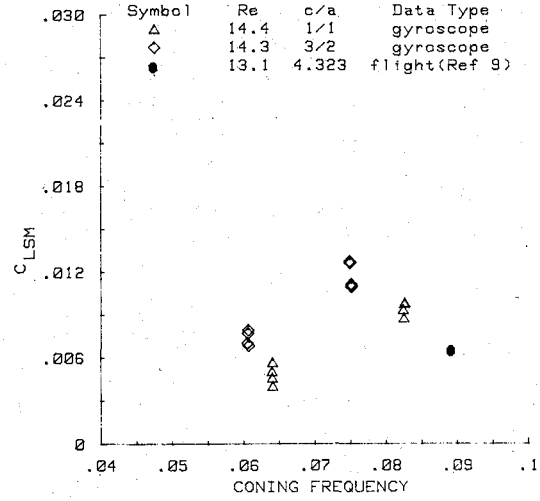

Fig. 11 Comparison of C_{LSM} for laboratory gyroscope and projectile flight for $Re \approx 14$.

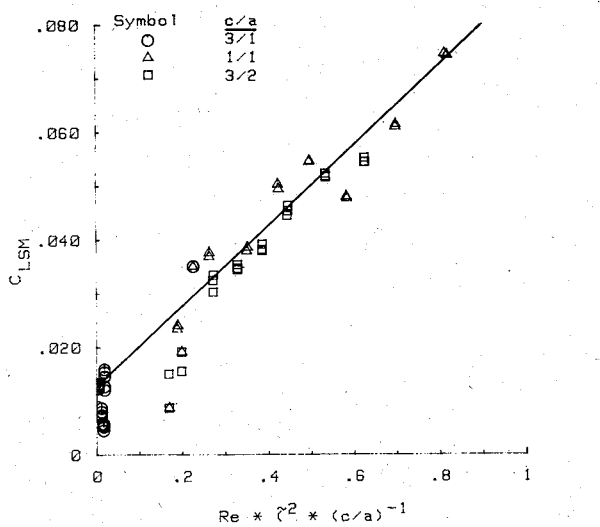

Fig. 10 Correlation of all data for viscosity ratios of 100,000 60,000, and 10,000 for C_{LSM} vs $Re \cdot \tau^2 \cdot (c/a)^{-4}$.

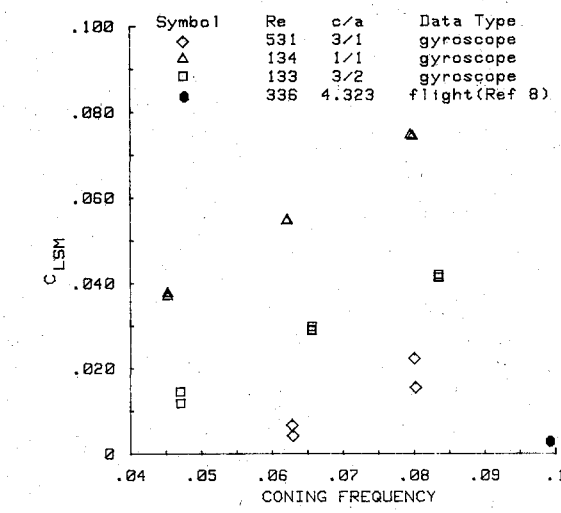

Fig. 12 Comparison of C_{LSM} for laboratory gyroscope and projectile flight for $133 < Re < 531$.

compared with the correlation suggested in Fig. 10. For $Re = 13.1$ and $C_{LSM} = 0.0153$, $(Re)\ (\tau)\ (c/a)^{-1} = 0.024$, while for $Re = 336$ and $C_{LSM} = 0.020$, $(Re)\ (\tau)\ (c/a)^{-1} = 0.76$. The $Re = 13.1$ datum falls close to the suggested correlation, but the $Re = 336$ datum does not agree with the correlation. The poor correlation of the $Re = 336$ datum could be atributed to the differences seen in Fig. 12 for the simple comparison of C_{LSM} vs τ.

Discussion

Yaw moments from the gyroscope can be readily displayed as simple functions of the Reynolds number. For data sets where c/a, ν, and $\dot{\phi}$ are constants, C_{LSM} can be averaged over all experimental values of τ, or,

$$C_{LSM_{ave}} = f(c/a, Re)$$

Figures 13a-c show $C_{LSM_{ave}}$ vs Reynolds number. The scales of these figures are identical to emphasize various aspects of the data. In Fig. 13a $C_{LSM_{ave}}$ dramatically increases as the Reynolds number increases. $C_{LSM_{ave}}$ does not decrease for extremely high Re values (as did the despin moment data of Miller). The resonance between the coning frequency and the liquid eigenfrequency for $c/a = 1/1$ only becomes stronger as Re increases. A similar situation exists for $c/a = 3/1$. However, the effects are much less obvious, as seen in Fig. 13b. The resonance with the liquid eigenfrequency is much weaker for $c/a = 3/1$ than for 1/1. The 3/2 cylinder was specifically chosen so as not to produce a resonance within the range of experimentally produceed coning frequencies. The yaw behavior for $c/a = 3/2$ indicates a maximum $C_{LSM_{ave}}$ for $Re \approx 100$, with smaller yaw moments for either larger or smaller Reynolds numbers (as in Fig. 13c). This type of behavior is similar in character to Miller's despin moment data.

A typical response curve for large Reynolds numbers is shown in Fig. 2. Response curves for lower Reynolds numbers show substantially reduced growth rates (Fig. 5). The predicted growth rates increase linearly with τ until the maximum growth rate is achieved. Also note from Figs. 2 and 3 that as the Reynolds number was reduced, the coning frequency for maximum growth rate increased. For $Re < 1{,}000$, the maximum growth rate may shift to $\tau < 0.1$. Thus, growth rates would increase linearly with coning frequency for $\tau < 0.1$. This is exactly what is observed. A continued reduction in Re will eventually give extremely large viscous damping and unstable yaw behavior will not be possible.

The previous rationale is not applicable to the 3/2 cylinder. Murphy[4] has shown that the average value of the liquid

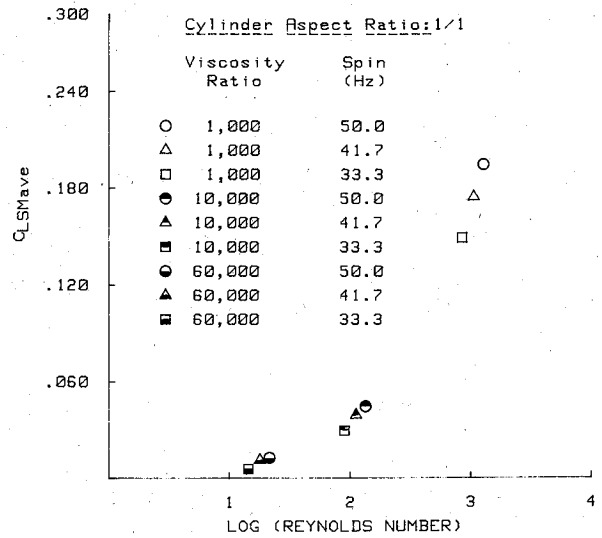

Fig. 13a Average C_{LSM} vs $\log_{10}(Re)$ for $c/a=1/1$.

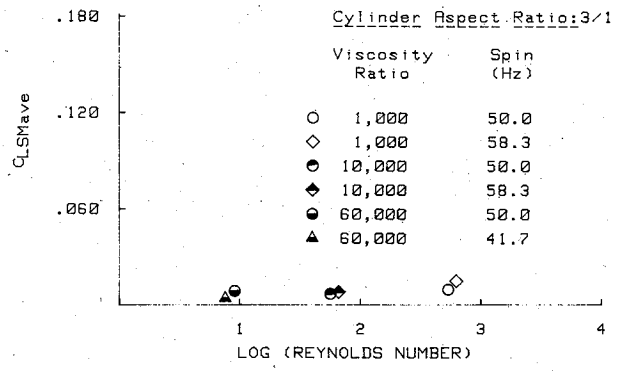

Fig. 13b Average C_{LSM} vs $\log_{10}(Re)$ for $c/a=3/1$.

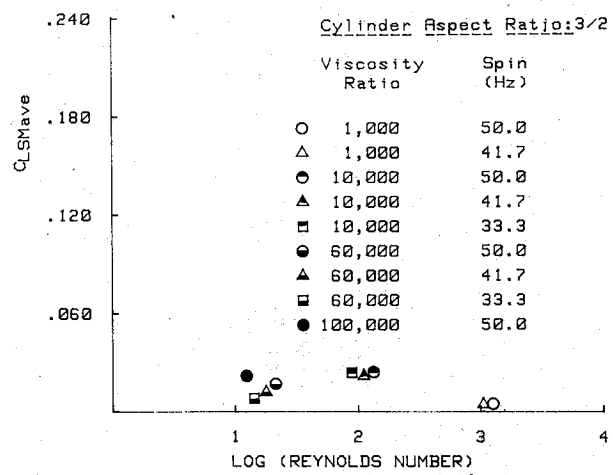

Fig. 13c Average C_{LSM} vs $\log_{10}(Re)$ for $c/a=3/2$.

moment is increased by a reduction in Re. Hence, for a nonresonant cylinder, such as $c/a=3/2$, large Re behavior is stable while low Re behavior could be unstable. When Re approaches unity, however, the liquid will act as a rigid body and no destabilizing effects will be observed. This mechanism is in qualitative agreement with the data for the 3/2 cylinder as shown in Fig. 13c.

Summary

Comparisons between gyroscope data and theory were consistent for $c/a=1/1$ for Reynolds numbers as small as 1010, but comparisons were inconsistent for $c/a=3/1$ when $Re=5210$. This indicates that theoretical models with viscous corrections of order $Re^{-1/2}$ may have an aspect ratio limit when the Reynolds number approaches 1000. Yaw moments for highly viscous flows are probably not generated from a new mechanism, but rather are the remnants of high Reynolds number resonances. However, the liquid-induced yaw moments are sufficiently large for $10<Re<100$ to destabilize motion of a spinning projectile or satellite.

References

[1] Stewartson, R., "On the Stability of a Spinning Top Containing Liquid," *Journal of Fluid Mechanics,* Vol. 5, 1959, pp 557-592.

[2] Wedemeyer, E.H., "Viscous Corrections to Stewartson's Stability Criterion," Ballistic Research Laboratory, Aberdeen Proving Ground, Md., BRL Rept. 1325, June 1966.

[3] Karpov, B.G., "Liquid-Filled Gyroscope: The Effect of Reynolds Number on Resonance," Ballistic Research Laboratory, Aberdeen Proving Ground, Md., BRL Rept. 1302, Oct. 1965.

[4] Murphy, C.H., "Angular Motion of a Spinning Projectile With a Viscous Liquid Payload," *Journal of Guidance, Control, and Dynamics,* Vol. 6, July-Aug. 1983, pp. 280-286.

[5] Gerber, N. and Sedney, R., "Moment on a Liquid-Filled Spinning and Nutating Projectile: Solid Body Rotation," Ballistic Research Laboratory, Aberdeen Proving Ground, Md., ARBRL-TR-02470, Feb. 1983.

[6] D'Amico, W.P. and Miller, M.C., "Flight Instability Produced by a Rapidly Spinning, Highly Viscous Liquid," *Journal of Spacecraft and Rockets,* Vol. 16, Jan.-Feb. 1979, pp. 62-64.

[7] Miller, M.C., "Flight Instabilities of Spinning Projectiles Having Non-Rigid Payloads," *Journal of Guidance, Control, and Dynamics,* Vol. 5, March-April 1982, pp. 151-157.

[8] D'Amico, W.P., Clay, W.H., and Mark, A., "Diagnostic Tests for Wick-Type Payloads and High Viscosity Liquids," Ballistic Research Laboratory, Aberdeen Proving Ground, Md., ARBRL-MR-02913, April 1979.

[9] D'Amico, W.P. and Clay, W.H., "High Viscosity Liquid Payload Yawsonde Data for Small Launch Yaws," Ballistic Research Laboratory, Aberdeen Proving Ground, Md., ARBRL-MR-03029, June 1980.